

© 2010 Prasad Shriram Sumant

INTERCONNECT CAPACITANCE EXTRACTION UNDER GEOMETRIC
UNCERTAINTIES

BY

PRASAD SHRIRAM SUMANT

THESIS

Submitted in partial fulfillment of the requirements
for the degree of Master of Science in Electrical and Computer Engineering
in the Graduate College of the
University of Illinois at Urbana-Champaign, 2010

Urbana, Illinois

Adviser:

Professor Andreas C. Cangellaris

Abstract

Interconnects are an important constituent of any large scale integrated circuit, and accurate interconnect analysis is essential not only for post-layout verification but also for synthesis. For instance, extraction of interconnect capacitance is needed for the prediction of interconnect-induced delay, crosstalk, and other signal distortion related effects that are used to guide IC routing and floor planning. The continuous progress of semiconductor technology is leading ICs to the era of 45 nm technology and beyond. However, this progress has been associated with increasing variability during the manufacturing processes. This variability leads to stochastic variations in geometric and material parameters and has a significant impact on interconnect capacitance. It is therefore important to be able to quantify the effect of such process induced variations on interconnect capacitance.

In this thesis, we have worked on a methodology towards modeling of interconnect capacitance in the presence of geometric uncertainties. More specifically, a methodology is proposed for the finite element solution of Laplace's equation for the calculation of the per-unit-length capacitance matrix of a multi-conductor interconnect structure embedded in a multi-layered insulating substrate and in the presence of statistical variation in conductor and substrate geometry. The proposed method is founded on the idea of defining a single, mean geometry, which is subsequently used with a single finite element discretization, to extract the statistics of the interconnect capacitance in an expedient fashion. We demonstrate the accuracy and efficiency of our method through its application to the extraction of capacitances in some representative geometries for IC interconnects.

To my family

Acknowledgments

This thesis is a product of my rewarding stay at UIUC for my Ph.D. in Mechanical Engineering and M.S. in Electrical Engineering. During my graduate studies, I have been privileged to work under the guidance of Prof. Andreas Cangellaris. I have a mechanical engineering background, but Prof. Cangellaris introduced me to the world of computational electromagnetics. He provided me with constant guidance and encouragement, and showed a lot of faith and patience during the course of my work. He was always available for discussions and allowed me a lot of freedom in pursuing various research ideas. I also got the opportunity to collaborate with a number of people during my stay at UIUC. I believe all this has helped me mature into a better person and a better researcher. Apart from academics, I have enjoyed many discussions and interactions with him on a number of topics. I wish to express my sincere gratitude to him, and I look forward to his continued guidance and advice in the future.

I would like to thank Prof. Aluru, who is my co-adviser for my Ph.D. work at UIUC, for his support, guidance and encouragement. Prof. Aluru always encouraged my interests in electromagnetics. He was always available for discussions and provided me with interesting ideas of approaching the given problem. I wish to express my sincere thanks to him.

I would like to thank Dr. Hong Wu, who mentored me when I joined UIUC. I have learned many things from him, including practical skills such as good programming practices. I would like to thank all current and former members of Prof. Cangellaris's research group. I enjoyed collaborating with Mr. Martien Oppeneer and cherish my time spent with him.

This research was supported in part by the Defense Advanced Research Projects Agency

(DARPA), under the N/MEMS Science and Technology Fundamentals Research Program and I would like to thank them for their support.

I wish to express my sincere thanks to Laurie Fisher, Beth Anne Rutledge and Doris Bonnett for their help and support over the years. I would like to thank Jamie Hutchinson and Janet Peters for carefully reviewing my thesis.

During the course of my stay at UIUC, I have made many good friends and I would like to thank them for making my stay enjoyable. I especially cherish my time spent with Rajan and Anjan, whether in lively debate on contentious topics or playing tennis. I would like to thank my fellow members of the Tae Kwon Do club and especially my instructor Candice, who has been a great motivator and a mentor outside of my academic life.

Finally, I would like to thank my family - my parents and my brother who have been a source of constant support and encouragement. And last but not least, I thank my wife Radhika, who incidentally is also a graduate student at UIUC. She has been a tremendous source of strength for me - particularly during tough times. I believe that her love and support have carried me through. It is not an overstatement to say that this work would not have been possible without her.

Table of Contents

List of Tables	vii
List of Figures	viii
Chapter 1 Introduction	1
1.1 Motivation and Literature Review	1
1.2 Thesis Objectives and Contributions	4
Chapter 2 Deterministic Capacitance Extraction	6
2.1 Basics of Capacitance Extraction	6
2.2 Survey of Capacitance Extraction Techniques	8
2.3 Finite Element Based Capacitance Extraction	9
Chapter 3 Stochastic Capacitance Extraction	12
3.1 Mathematical Formulation	12
3.1.1 Mapping	12
3.1.2 Visualization of the position-dependent flux line	16
3.2 Computer Implementation	18
3.2.1 Polynomial chaos approach	18
3.2.2 Monte Carlo or stochastic collocation approach	21
3.3 Numerical Studies	21
3.3.1 Example 1: Single conductor over a ground plane	22
3.3.2 Example 2: Strip conductor interconnect in a multi-layered dielectric substrate	25
3.3.3 Example 3: Two strip conductors over a ground plane	26
3.3.4 Example 4: A three-conductor interconnect over a ground plane	26
3.4 Summary	28
References	30
Author's Biography	33

List of Tables

3.1	Example 1 (self-capacitance in pF/cm): Statistical change in G	24
3.2	Example 1 (self-capacitance in pF/cm): Statistical change in L	25
3.3	Example 2 (self-capacitance in pF/cm): Statistical change in thicknesses	26
3.4	Example 3 (self-capacitance in pF/cm): Statistical change in H and S	26
3.5	Example 4: Mean capacitance in pF/cm using standard Monte Carlo and our proposed approach	28
3.6	Example 4: Standard deviation of self-capacitance in pF/cm using standard Monte Carlo and our proposed approach	28

List of Figures

2.1	Parallel plate capacitor.	7
2.2	Schematic of a 3D interconnect structure.	8
2.3	Cross-sectional and top views of interconnect.	8
2.4	Cross-sectional geometry of a configuration of a set of parallel conductors embedded in a multi-layer dielectric domain.	10
2.5	A two-conductor configuration with conductor C_1 taken as the active conductor, while conductor C_2 is taken as the reference.	11
3.1	Definition of the mean cross section and the cross section of one random sample geometry.	13
3.2	Position-dependent flux-line lengths in mean and random geometry.	17
3.3	(a) One conductor over a ground plane. (b) Probability distribution function of the capacitance for a 10% variation in distance from ground plane.	23
3.4	Strip conductor embedded in multiple dielectrics.	25
3.5	Two conductors over a ground plane.	27
3.6	Three conductors over a ground plane.	27

Chapter 1

Introduction

1.1 Motivation and Literature Review

Interconnects are an important constituent of any large scale integrated (LSI) circuit. The continuous progress of semiconductor technology is leading ICs to the era of 45 nm technology and beyond. This nanometer technology scaling has enabled designers to integrate more functionality on the chip. Active device counts are reaching hundreds of millions. Interconnect dimensions are being scaled with the devices whenever possible. However, this scaling has created problems with signal integrity and interconnect delay. Furthermore, the use of new device structures and an increasing number of metal layers are introducing millions of new parasitic effects in designs. Interconnect, which was once considered just a parasitic, can now be a dominant factor for integrated circuit performance. For instance, interconnect and device parasitic effects are estimated to account for over 60 percent of the delay at 28 nm. Consequently, accurate interconnect analysis has become essential not only for post-layout verification but also for synthesis. For instance, extraction of interconnect capacitance is needed for the prediction of interconnect-induced delay, crosstalk, and other signal distortion related effects that are used to guide IC routing and floor planning. Over the past decade there have been a number of advances in modeling and analysis of interconnect that have facilitated the continual advances in design automation of systems of increasing size and frequency.

With migration of VLSI circuits toward deep submicron dimensions, variability during manufacturing processes has assumed significant importance. Interconnect variability arises

in the lithography process and other processes such as etching and chemical mechanical polishing (CMP). Such process-induced variations lead to random variations in geometry and material properties of the interconnect. To determine the extent of such effects, the distribution of various electrical parameters, such as interconnect resistances and capacitances, must be determined. Such distribution can then be used for considering interconnect variability in a design flow, particularly in parasitic extraction [22], [19] and signal-integrity [18] and timing analyses [28], [6].

In general, there are three broad ways of handling randomness or uncertainty in physical domains: Monte Carlo based approaches, orthogonal polynomial chaos expansions and stochastic collocation based methods. These are briefly reviewed in the following.

A standard way to capture the impact of random variations in conductor geometry and material properties on capacitance value is through brute-force Monte Carlo computation [12]. In such an approach, one considers a large number (typically greater than 10000) of realizations (or samples) of the geometry, and a deterministic problem is solved for each one of these realizations. The generated data is then used for the development of the statistics, such as the mean and standard deviation, of the capacitance. Clearly, such an approach is time-consuming, with a convergence rate in obtaining reliable statistics of $O(N^{-1/2})$, where N is the number of samples used. Several techniques have been developed for improving convergence of the Monte Carlo process. Among them we mention the Latin hypercube sampling [23],[30], the quasi-Monte Carlo (QMC) method, [13], [26], [27], and the Markov chain Monte Carlo method (MCMC) [15]. In [4], the standard random-walk based solver was extended to take into account the statistical models of these variations. The variations were handled by additional Monte Carlo sampling.

In terms of non-statistical approaches, Ghanem and Spanos [14] developed the polynomial chaos approach. Polynomial chaos is a spectral expansion of the stochastic processes in terms of the orthogonal polynomials as given by Wiener's homogeneous chaos theory. When the underlying random variables are Gaussian, a homogeneous chaos expansion us-

ing Hermite polynomials leads to fast convergence. The idea was generalized by Xiu and Karniadakis to account for uncertainty in the numerical modeling of a variety of physical phenomena, such as diffusion [35] and fluid flow [36]. More recently, [1] [2], the polynomial chaos theory was used in the context of a Lagrangian boundary element method (BEM) for performing electrostatic and coupled electro-mechanical analysis of MEMS systems. One of the shortcomings of polynomial chaos is that the dimension of the problem grows very quickly as the number of random inputs increases. Also, the resulting system of deterministic equations that constitutes the approximate problem is coupled and this adds to the computational overhead of the solution. In [11], a novel statistical capacitance extraction method for interconnects considering process variations was proposed. The new method, called statCap, was based on the spectral stochastic method where orthogonal polynomials are used to represent the statistical processes in a deterministic way. In [16], a fast-multipole method (FMM) was presented for a parallel and incremental full chip capacitance extraction considering stochastic variation, namely piCAP. In this approach, the process variations were modeled using stochastic orthogonal polynomials.

The stochastic collocation method [34],[8],[3] tries to combine the advantages of both stochastic Galerkin methods and classical Monte Carlo approaches. The key idea is to use a “decoupled” polynomial interpolation in multi-dimensional random space. Lagrange interpolation is one such example; thus, what is required is a run of the deterministic solver for each point in the multi-dimensional parameter space. These interpolation points in random space can be generated using various algorithms such as Strouds cubature and Smolyak sparse grids [29]. Compared to stochastic Galerkin methods, collocation methods generally result in a larger number of equations; however, these equations are easier to solve as they are completely decoupled and require only repetitive runs of a deterministic solver. Stochastic collocation is also more efficient than brute force Monte Carlo due to the smart choice of the interpolation points. A spectral stochastic collocation method was proposed for the capacitance extraction of interconnects with geometric stochastic variations

in [38]. Boundary element method (BEM) was the method used for deterministic capacitance extraction. In [37], an efficient method was proposed to consider the process variations with spatial correlation, for chip-level capacitance extraction based on the window technique. In each window, an efficient technique of Hermite polynomial collocation (HPC) was presented to extract the statistical capacitance.

In [21], an efficient methodology was presented for generating explicit statistical representations of parasitic capacitances. The methodology makes use of principle factor analysis to reduce the number of random variables while preserving the dominant global/local factors that induce the conductor surface fluctuation due to process variations. In [39], an approach to account for the impact of conductor surface roughness on capacitance was presented.

1.2 Thesis Objectives and Contributions

The method presented in this paper is aimed at the extraction of the per-unit-length capacitance matrix, in the presence of geometric uncertainty, of multi-conductor interconnect geometries embedded in multi-layered, dielectrics. A number of numerical methods are used for computation of deterministic capacitance. We review these in Chapter 2. Integral equation solvers, accelerated through the use of fast iterative techniques like the multipole method, have been among the most popular solvers [25]. However, for the case of conductors embedded in inhomogeneous dielectrics, the efficiency of random walk-based methods [20],[10] has made them a popular method of choice. Arbitrary material inhomogeneity is also handled efficiently by finite element methods. For the purposes of this thesis, the finite element method will be used for the solution of the electrostatic BVP [32]. The objective of this work is to demonstrate a finite-element based methodology for the fast extraction of the per-unit-length capacitance matrix of a multi-conductor interconnect in the presence of stochastic variations in its cross-sectional geometry.

As already mentioned above, in the context of stochastic collocation or Monte Carlo,

the solution of the boundary value problems (BVPs) in the presence of statistical variations in geometry and material parameters requires the solution of a number of deterministic problems for a set of samples of the uncertain geometry. Thus, in the context of finite element methods, for each sample, a new finite element mesh and a corresponding system of linear equations has to be generated. This makes the stochastic analysis computationally expensive. The methodology proposed is aimed at overcoming this complexity hurdle. The main idea of the proposed method is to use one or two deterministic runs of the underlying problem for generating sufficient information for performing stochastic analysis. Toward this objective we need to rely on the definition of a single “reference” geometry, the one that will be discretized using the finite element method, and then develop “mappings” from each of the random samples to the reference geometry. This way we eliminate the need to generate a new finite element model for each one of the sample problems to be solved. Also, the deterministic problem to be solved is the one on the reference geometry and it is uncoupled. We describe this methodology in Chapter 3.

Chapter 2

Deterministic Capacitance Extraction

In this chapter, we begin with an introduction to the basics of capacitance extraction of interconnects. It is followed by a brief survey of various methods for modeling interconnect capacitance. Finally, we present the formulation for finite element based computation of interconnect capacitance.

2.1 Basics of Capacitance Extraction

An interconnect is a wire that provides a conductive path between different functional elements such as gates, devices etc. Ideally it should not affect design performance. However, real wire has resistance, inductance and capacitance. Wiring forms a complex geometry and introduces resistive, inductive and capacitive effects that impact delay, energy consumption and power distribution. It is therefore important to be able to model these effects. The focus of this thesis is on interconnect capacitance.

The simplest model to describe capacitance is using a parallel plate capacitor. It consists of two metal plates separated by a distance d and at potentials of Φ_1 and Φ_2 (Fig. 2.1). The medium between the two metal plates is a dielectric of permittivity ϵ . A charge of $+Q$ and $-Q$ is distributed on the two plates. Capacitance, which is defined as the capacity to store charge, is then calculated as

$$C = \frac{Q}{V} \tag{2.1}$$

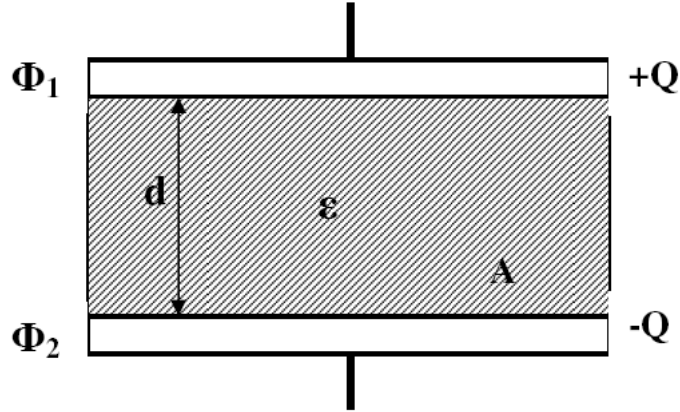


Figure 2.1: Parallel plate capacitor.

In terms of geometric and material parameters, it is obtained as

$$C = \epsilon \frac{A}{d} \quad (2.2)$$

This simple relationship reveals a lot of information for developing an intuitive understanding of capacitance. For example, it describes how the geometry of the two metal plates impacts capacitance. It is clear that a stochastic variation in area A or the gap d can cause a stochastic variation in capacitance.

In practice, the interconnect structures are very complicated (Fig. 2.2). Shown in Fig. 2.3 are top views and cross-sectional views of the interconnect structure. For an N conductor system, a capacitance matrix is defined,

$$[Q] = [C] [V] \quad (2.3)$$

where $[C]$ is the capacitance matrix, C_{ii} represents self-capacitance while C_{ij} represents mutual capacitance.

In the next section, we will look at various techniques used for computing the capacitance matrix.

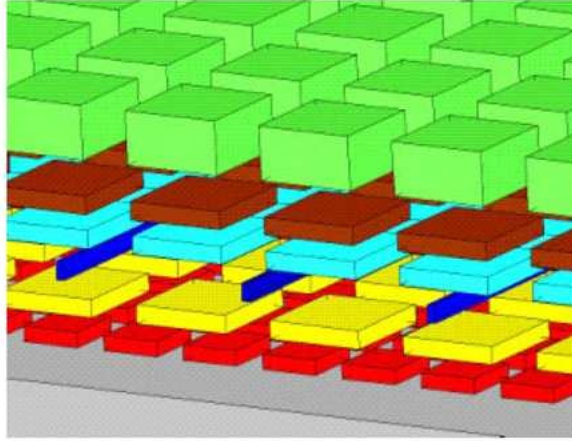


Figure 2.2: Schematic of a 3D interconnect structure.

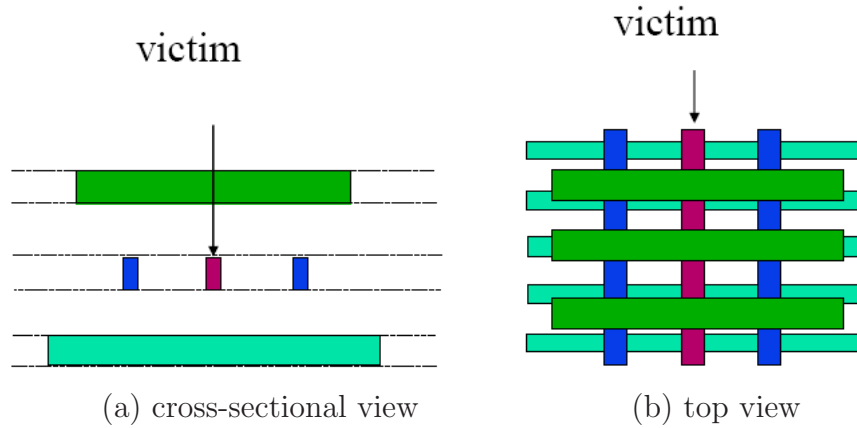


Figure 2.3: Cross-sectional and top views of interconnect.

2.2 Survey of Capacitance Extraction Techniques

There are many techniques for computing the interconnect capacitance matrix. They can be subdivided into geometrical and numerical methods. Geometrical methods have evolved from simple parallel-plate calculations into elaborate geometric models to include more and more fringing effects [5]. Basically, they are fitting formulas, of which the coefficients are determined by numerical calculations or sometimes by measurements. All modern extractors (e.g.[33],[24],[7]) use such methods, and the fitting coefficients can be determined by automated procedures from a file with layer thicknesses and permittivities. Because of their ability to model certain coupling capacitances, these methods are sometimes called quasi-3D

methods. Such methods are fast, and to a certain extent they can predict the capacitances fairly well. However, designers sometimes want to check the results of those quasi-3D calculations against numerical calculations that start from first principles. Although it might not be feasible to do this for a full chip, some critical parts of the layout can be analyzed in more detail.

Common numerical techniques include the finite-difference method (FDM) [17], the finite-element method (FEM) [9] and the boundary-element method (BEM) [25]. In both the FDM and the FEM, the external field is discretized. Because this field in principle extends to infinity, it has to be truncated using a bounding box. These methods typically lead to large but sparse systems of equations.

In the BEM, on the other hand, only the boundary of the field region is discretized. Hence, the 3D problem is effectively reduced to a 2D problem. The resulting matrix is therefore much smaller, but full. Boundary element methods are most effective when the medium is regular, or in the capacitance extraction case, when the chips have a stratified dielectric structure. To a certain extent, this is usually the case because of planarization. However, for the case of conductors embedded in inhomogeneous dielectrics, the efficiency of random walk-based methods [20],[10] has made them a popular method of choice.

Arbitrary material inhomogeneity is also handled efficiently by finite element methods. In this thesis, we make use of the finite element method for modeling interconnect capacitance. In the following section, we describe its formulation.

2.3 Finite Element Based Capacitance Extraction

As depicted in Fig. 2.4, the geometry under consideration consists of a number of conductors embedded in a stack of dielectric layers. Capacitance extraction for the multi-conductor geometry involves the solution of a set of electrostatic boundary value problems. To fix ideas, consider a configuration of N *active* conductors and one or more conductors used as

reference conductors, with respect to whom the potential of each one of the N conductors is defined. For such a configuration, N electrostatic boundary value problems are solved for the extraction of the so-called $N \times N$ short-circuit capacitance matrix of the N active conductors. For the i -th boundary value problem, active conductor i is set at potential of 1 V, with all remaining active conductors, along with the reference conductors, set at zero potential.

As the geometry in Fig. 2.4 suggests, the geometric and material properties of the structures considered in this paper are assumed to be invariant in one of the three directions in the reference Cartesian coordinate system. Thus, the boundary value problem of interest is a two-dimensional (2-D) one and its solution necessitates the discretization of the cross-sectional geometry of the structure on a plane perpendicular to the axis of invariance.

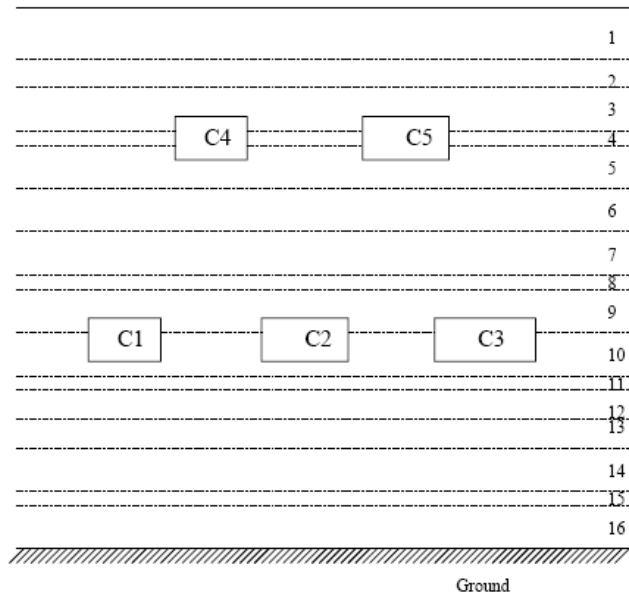


Figure 2.4: Cross-sectional geometry of a configuration of a set of parallel conductors embedded in a multi-layer dielectric domain.

Without loss of generality, we choose to present the mathematical formulation of our methodology for the simple configuration depicted in Fig. 2.5. The objective is the solution of Laplace's equation

$$\nabla^2 \phi = 0 \tag{2.4}$$

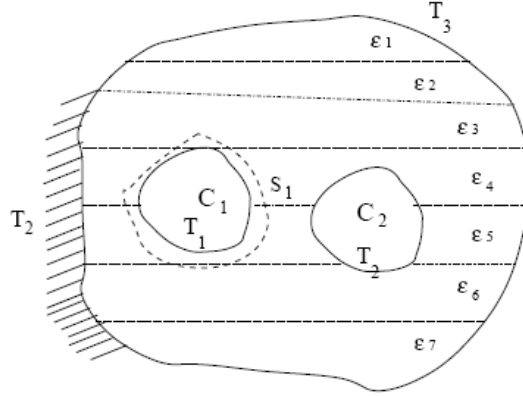


Figure 2.5: A two-conductor configuration with conductor C_1 taken as the active conductor, while conductor C_2 is taken as the reference.

for the electrostatic potential ϕ , subject to the following three types of boundary conditions T_1 , T_2 and T_3 on various segments of the problem domain:

$$\phi = 1 \quad \text{on} \quad T_1 \quad (2.5)$$

$$\phi = 0 \quad \text{on} \quad T_2 \quad (2.6)$$

$$\frac{\partial \phi}{\partial n} = 0 \quad \text{on} \quad T_3 \quad (2.7)$$

Thus, for this configuration, conductor C_1 is the active conductor while C_2 is the reference conductor. In addition to the aforementioned boundary conditions, the conditions of potential and electric flux density ($-\epsilon \nabla \phi$) continuity at dielectric interfaces are imposed.

The numerical solution of the aforementioned boundary value problem (BVP) will be obtained using FEM. The per-unit-length capacitance, C , is calculated, subsequently, through the integral

$$C = - \int_S \epsilon \frac{\partial \phi}{\partial n} dl \quad (2.8)$$

where the integration is carried out over an appropriate Gaussian contour S that encloses the active conductor and is placed in its immediate vicinity. The unit normal, \hat{n} , is taken to be pointing outwards from the Gaussian contour.

Chapter 3

Stochastic Capacitance Extraction

In this chapter, we present our proposed method for extraction of interconnect capacitance under uncertainty.

3.1 Mathematical Formulation

In this section we describe the physical motivation and mathematical foundation for the proposed approach. First, we describe a method for developing a “mapping” from a random sample to a reference geometry. As we will describe in the following, the reference geometry is the *mean* geometry. This mapping allows us to compute the solution for the electrostatic problem for each one of the samples from the solution in the mean geometry. We describe how the stochastic electrostatic analysis is performed. Finally, a simple example geometry is considered that provides a visualization of the “mapping.”

3.1.1 Mapping

Our approach for the development of the mapping is the one first described in [31] in the context of electrostatic modeling of MEMS devices. We will facilitate the discussion with the aid of Fig. 3.1. The figure depicts the cross-sectional geometry of a two-conductor interconnect structure, where the assumption is made that the cross-sectional geometry remains constant along the interconnect axis. Hence, the BVP under consideration is the one for calculating the per-unit-length capacitance of the interconnect. Without loss of generality the reference conductor is taken to be a ground plane with fixed cross-sectional

geometry. However, as the numerical examples demonstrate, the proposed methodology is general and allows for variability in all conductor geometries. The conductors are embedded in a dielectric medium, with position-dependent relative permittivity over the interconnect cross section. Two different cross-sectional geometries are shown for the conductor. The one with the solid line denotes the mean conductor cross section while the one with the dotted line denotes the cross section of one random sample. This random sample is the result of statistical variation in the cross section of the conductor and/or its position with respect to the reference ground plane. Also shown in the figure are electric flux lines, one for each one of the two cross-sectional geometries, starting from the conductor and terminating on the ground plane. At both ends each flux line is perpendicular to the conducting surfaces. Furthermore, the starting point P' of the flux line on the random sample cross section is taken to be the point at which the flux line starting from point P on the mean cross section intersects the random sample cross section.

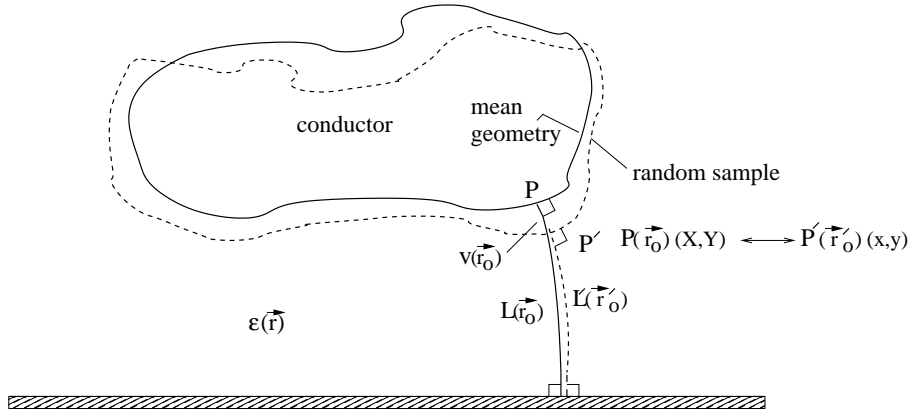


Figure 3.1: Definition of the mean cross section and the cross section of one random sample geometry.

Consider the electric flux line L' (Fig. 3.1) starting at point $P'(\vec{r}'_0)(x,y)$ on the random sample conductor. Let V_0 be the conductor voltage with respect to the ground. Along the electric flux line the magnitude of the electric flux density $\vec{D}'(\vec{r}')$ is constant, equal to $|\vec{D}_c|$.

Hence, we can write

$$\int_{L'} \vec{E} \cdot d\vec{l} = V_0 \quad (3.1)$$

$$\int_{L'} \frac{\vec{D}'(\vec{r}') \cdot d\vec{l}'}{\epsilon(\vec{r}')} = V_0 \quad (3.2)$$

$$|\vec{D}_c| \int_{L'} \frac{1}{\epsilon(\vec{r}')} dl' = V_0 \quad (3.3)$$

$$|\vec{D}'(\vec{r}_0')| = |\vec{D}_c| = \frac{V_0}{\int_{L'} \frac{1}{\epsilon(\vec{r}')} dl'} \quad (3.4)$$

In a similar manner, the line integral of the electric field along a flux line L between the ground plane and point $P(\vec{r}_0)(X, Y)$ on the surface of the mean cross section conductor yields the following:

$$|\vec{D}(\vec{r}_0)| = \frac{V_0}{\int_L \frac{1}{\epsilon(\vec{r})} dl} \quad (3.5)$$

From (3.4) and (3.5) we have

$$|\vec{D}'(\vec{r}_0')| = Q |\vec{D}(\vec{r}_0)| \quad (3.6)$$

$$Q = \frac{\int_L \frac{1}{\epsilon(\vec{r})} dl}{\int_{L'} \frac{1}{\epsilon(\vec{r}')} dl'} \quad (3.7)$$

It is noted that the above equation, which is exact, establishes a linear relationship between the charge density at a point on the surface of the mean cross section of the conductor and that at a point on the surface of the cross section of one of the random samples. Furthermore, it is important to note that, under the assumption of sufficiently small perturbations of the random sample cross section from the mean cross section, and provided that the points $P'(\vec{r}_0')$ and $P(\vec{r}_0)$ are selected in a manner such that $P'(\vec{r}_0')$ is the point at which the flux line L starting at point $P(\vec{r}_0)$ intersects the surface of the cross section of the random sample, the above expressions can be manipulated in a manner such that the ratio Q can be

approximated in an accurate and expedient fashion. The way this is done is described next.

Using (3.5) a position-dependent, flux line length, $G(\vec{r}_0)$, associated with each point along the boundary of the mean cross section, may be defined as

$$G(\vec{r}_0) = \epsilon(\vec{r}_0) \frac{V_0}{\left| \vec{D}(\vec{r}_0) \right|} \quad (3.8)$$

where $\epsilon(\vec{r}_0)$ is the electric permittivity adjacent to the conductor at point $P(\vec{r}_0)$, while $\left| \vec{D}(\vec{r}_0) \right|$ is the magnitude of the electric charge density on the conductor at that point. It is noted that $G(\vec{r}_0)$ can be computed for all points on the mean cross section from the solution of the electrostatic BVP with the voltage on the mean conductor cross section set at V_0 .

Returning to the random sample cross section, the length $L'(\vec{r}_0')$, in view of the discussion above, may be approximated as

$$L'(\vec{r}_0') \approx L(\vec{r}_0) - v(\vec{r}_0) \quad (3.9)$$

where, as depicted in Fig. 3.1, $v(\vec{r}_0)$ is the length of the flux line L between points $P(\vec{r}_0)$ and $P'(\vec{r}_0')$. Using (3.4),(3.5) and (3.8), we have

$$\int_L \frac{1}{\epsilon(\vec{r})} dl = \frac{G(\vec{r}_0)}{\epsilon(\vec{r}_0)} \quad (\text{exact}) \quad (3.10)$$

$$\int_{L'} \frac{1}{\epsilon(\vec{r}')} dl' \approx \int_{L-v} \frac{1}{\epsilon(\vec{r})} dl \quad (3.11)$$

$$\begin{aligned} \int_{L'} \frac{1}{\epsilon(\vec{r}')} dl' &\approx \int_L \frac{1}{\epsilon(\vec{r})} dl - \int_v \frac{1}{\epsilon(\vec{r})} dl \\ &= \frac{G(\vec{r}_0)}{\epsilon(\vec{r}_0)} - \frac{v(\vec{r}_0)}{\epsilon(\vec{r}_0)} \end{aligned} \quad (3.12)$$

Thus, (3.7) becomes

$$\left| \vec{D}'(\vec{r}_0') \right| \approx \left| \vec{D}(\vec{r}_0) \right| \frac{G(\vec{r}_0)}{G(\vec{r}_0) - v(\vec{r}_0)} \quad (3.13)$$

This is the final expression relating charge density on the random sample conductor surface to the charge density on the mean conductor surface. It describes the required, position-dependent *mapping* from a random sample to a mean geometry. Clearly, $G'(\vec{r}'_0) = G(\vec{r}_0) - v(\vec{r}_0)$ can be interpreted as the approximation of the position-dependent, flux line length in the random sample conductor cross section. The accuracy of this approximation is discussed in detail in [31].

The capacitance per unit length of the random sample cross section is calculated through the integral

$$C' = \int_{C_{rs}} |\vec{D}'(\vec{r}')| dl' \quad (3.14)$$

$$C' = \int_{C_{mean}} \frac{G(\vec{r})}{G(\vec{r}) - v(\vec{r})} |\vec{D}_0(\vec{r})| |J| dl \quad (3.15)$$

where J is the Jacobian of the map between the random sample cross section and the mean cross section. C_{rs} , C_{mean} denote, respectively, the contour of the random sample cross section and the mean cross section. The Jacobian can be computed using

$$J = \begin{bmatrix} \frac{\partial x}{\partial X} & \frac{\partial y}{\partial X} \\ \frac{\partial x}{\partial Y} & \frac{\partial y}{\partial Y} \end{bmatrix} \quad (3.16)$$

Thus, we have a way to compute capacitance of the random sample from the solution for charge density on the mean sample.

3.1.2 Visualization of the position-dependent flux line

In order to visualize how the flux lines change as the geometry undergoes small statistical variations, let us consider a simple example. The geometry is depicted in Fig. 3.2. The problem consists of a unit square conductor embedded in a dielectric within another square conductor with sides of dimension 2. The unit square is at a potential 1.0 while the enclosing

conductor is at potential 0. Also shown in Fig. 3.2 is the location of the unit square under two configurations: the mean configuration, shown in blue circles, and a random sample realization, shown in red squares. Let us now consider two points A and B at two different sections of the mean geometry. At point A , the mean geometry has a displacement that takes it closer to the boundary (A'). We would thus expect an increase in the electric field at point A or decrease in flux length, $L > L'$. From the numerical solution of the electrostatic problem in the two configurations we obtain $L = 0.49$, $L' = 0.45$ while $v = 0.05$. At point B , the mean geometry has a displacement that takes it away from the boundary B' . We would thus expect a decrease in the electric field at point B or increase in flux length, $L < L'$. Numerically, $L = 0.49$, $L' = 0.53$ while $v = 0.05$. These results are consistent with (3.9). While points A and B represent “most” of the points on the mean geometry, there are points particularly near the corners, where (3.9) will not be very accurate. Since the capacitance involves an averaging effect over the entire cross section, some of these errors are numerically canceled while some contribute to the error.

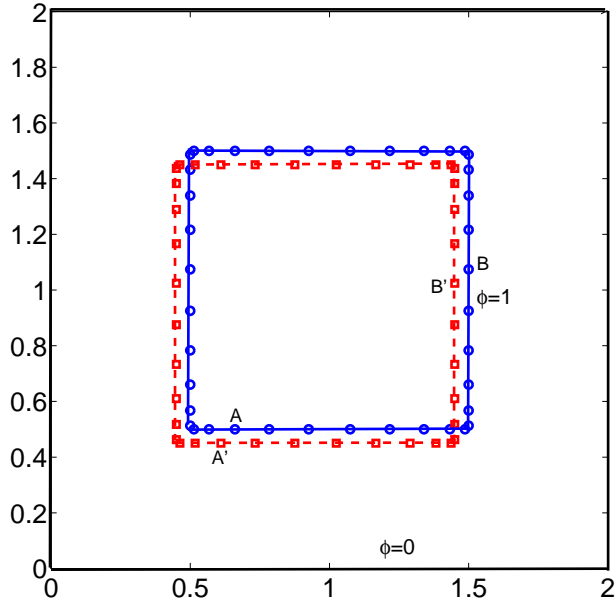


Figure 3.2: Position-dependent flux-line lengths in mean and random geometry.

3.2 Computer Implementation

In order to implement the proposed “mapping” approach in a computer simulation, we have to consider different methods of representing random geometry. In the following two subsections we consider an orthogonal polynomial chaos expansion and a statistical approach, such as Monte Carlo or stochastic collocation.

3.2.1 Polynomial chaos approach

Consider a deterministic domain D in \mathfrak{R}^d , $d = 1, 2$ and let $\vec{r} \in D$. Let $(\Omega, \mathfrak{S}, P)$ denote a probability space, where Ω is the set of all possible events, \mathfrak{S} is the σ -algebra of events and P is the probability measure. The symbol θ represents an event in Ω . Then, all real valued functions $\xi(\theta)$ defined on Ω are known as random variables, while functions $u(\vec{r}, \theta)$ defined on $D \otimes \Omega$ are known as random processes.

The polynomial chaos expansion is a spectral expansion of the random process in terms of the orthogonal polynomials in multi-dimensional random variables. For the purpose of this study, and without loss of generality, we assume that all inputs are Gaussian random variables. Thus, we consider Hermite polynomials of Gaussian random variables for expansion. Let $\{\xi_i(\theta)\}_{i=1}^{\infty}$ be a set of orthonormal Gaussian random variables. Using this, the polynomial chaos expansion of a second-order random process $u(\vec{r}, \theta)$ is given as [14]

$$u(\vec{r}, \theta) = \sum_{i=1}^{\infty} \mu_i(\theta) g_i(\vec{r}) \quad (3.17)$$

$$u(\vec{r}, \theta) = a_0(\vec{r}) \Gamma_0 + \sum_{i_1=1}^{\infty} a_{i_1}(\vec{r}) \Gamma_1(\xi_{i_1}(\theta)) \quad (3.18)$$

$$+ \sum_{i_1=1}^{\infty} \sum_{i_2=1}^{\infty} a_{i_1 i_2}(\vec{r}) \Gamma_2(\xi_{i_1}(\theta), \xi_{i_2}(\theta)) + \dots \quad (3.19)$$

where $\Gamma_n(\xi_{i_1}, \xi_{i_2}, \dots, \xi_{i_n})$ denotes the polynomial chaos of order n in terms of the multi-dimensional Gaussian random variables $\xi = (\xi_{i_1}, \xi_{i_2}, \dots, \xi_{i_n})$. For convenience, Eqn. (3.18) is

often rewritten as

$$u(\vec{r}, \theta) = \sum_{i=0}^{\infty} \hat{a}_i(\vec{r}) \Psi(\xi(\theta)) \quad (3.20)$$

where there is a one-to-one correspondence between the functions $\Gamma[\cdot]$ and $\Psi[\cdot]$ and between the associated coefficients. For the case of one-dimensional Hermite polynomial chaos, $\xi_1 = \xi$, and Ψ are the one-dimensional Hermite polynomials given as [14]

$$\Psi_0(\xi) = 1, \Psi_1(\xi) = \xi, \Psi_2(\xi) = \xi^2 - 1, \quad (3.21)$$

$$\Psi_3(\xi) = \xi^3 - 3\xi, \Psi_4(\xi) = \xi^4 - 6\xi^2 + 3, \dots \quad (3.22)$$

In practice, a finite number of random variables are used in the expansion to represent finite number of random parameters in the system. Also, the order of the polynomial used in the expansion is restricted to p . Thus, the expansion in Eqn. (3.19) can now be written as

$$u(\vec{r}, \theta) = \sum_{i=0}^N \hat{a}_i(\vec{r}) \Psi(\xi(\theta)) \quad (3.23)$$

The total number of terms included in the polynomial chaos expansion ($N + 1$) depends both on the dimensionality n and the highest order p of the multi-dimensional polynomials used, and is given as

$$N + 1 = \frac{(n + p)!}{n!p!} \quad (3.24)$$

Thus, a stochastic quantity is expanded in terms of orthogonal polynomials of random variables. The coefficients of these polynomials are functions of space. The stochastic quantity is well-defined once these coefficients are computed.

As discussed in Section 3.1.1, a random geometry can be modeled in terms of the mean

geometry and a random displacement $v(\vec{r}, \theta)$. Mathematically,

$$\tilde{G}(\vec{r}, \theta) = \overline{G}(\vec{r}) - v(\vec{r}, \theta) \quad (3.25)$$

Recall from Eqn. (3.13), the relationship

$$\left| \vec{D}'(\vec{r}') \right| \approx \left| \vec{D}_0(\vec{r}) \right| \frac{G(\vec{r})}{G(\vec{r}) - v(\vec{r})} \quad (3.26)$$

Using Taylor series expansion on the right-hand side above,

$$\left| \vec{D}'(\vec{r}) \right| \approx \left(1 + \frac{v(\vec{r})}{G(\vec{r})} + \frac{v(\vec{r})^2}{G(\vec{r})^2} + \frac{v(\vec{r})^3}{G(\vec{r})^3} + \dots \right) \left| \vec{D}_0(\vec{r}) \right| \quad (3.27)$$

Thus, in terms of stochastic quantities (Eqn. (3.23)),

$$\left| \tilde{D}(\vec{r}) \right| \approx \left(1 + \frac{v(\vec{r}, \theta)}{G(\vec{r})} + \frac{v(\vec{r}, \theta)^2}{G(\vec{r})^2} + \frac{v(\vec{r}, \theta)^3}{G(\vec{r})^3} + \dots \right) \left| \vec{D}_0(\vec{r}) \right| \quad (3.28)$$

From (3.15) and above, the stochastic capacitance can be written as

$$\tilde{C} = \int_S \left(1 + \frac{v(\vec{r}, \theta)}{G(\vec{r})} + \frac{v(\vec{r}, \theta)^2}{G(\vec{r})^2} + \frac{v(\vec{r}, \theta)^3}{G(\vec{r})^3} + \dots \right) |J| \vec{D}_0 \cdot d\vec{s} \quad (3.29)$$

The random displacement can be modeled using polynomial chaos,

$$v(\vec{r}, \theta) = \sum_{i=0}^N v_i(\vec{r}) \Psi(\xi(\theta)) \quad (3.30)$$

Using the same expansion for capacitance \tilde{C} ,

$$\tilde{C} = \sum_{i=0}^N C_i(\vec{r}) \Psi(\xi(\theta)) \quad (3.31)$$

The coefficients C_i can be easily computed using the above three relations. The important

point is that only a single deterministic run, the one for the mean geometry to compute \vec{D}_0 , is required. Once that is obtained, calculating the coefficients C_i is straightforward. The statistics of capacitance can be easily computed once these coefficients have been obtained. In the numerical examples section, the pertinent process will be explained in more detail with the help of an example.

3.2.2 Monte Carlo or stochastic collocation approach

In this section, we will look at how our proposed approach can be used in conjunction with other methods for representing random geometry - statistical approaches such as Monte Carlo or stochastic collocation. In these approaches, one considers many realizations of random geometry. For our proposed method, we consider the mean geometry and perform finite element solution on this mean geometry to compute position-dependent $G(\vec{r})$. Next, for each random realization of the geometry, we compute $v(\vec{r})$ which is the displacement of the random geometry from the mean. It is important to note that this calculation does not require any finite element discretization. Thus, for each random geometry, capacitance is computed using (3.15). Once all capacitances C_i have been computed, it is easy to compute the desired statistics such as mean and standard deviation. Use of statistical methods such as Monte Carlo or stochastic collocation is particularly useful when the number of input random variables is large, because for such cases, the orthogonal polynomial expansion grows in size and complexity. We demonstrate this approach in the numerical studies section using one example.

3.3 Numerical Studies

In this section, we consider some representative problems for demonstrating the accuracy and efficiency of our proposed method. All geometries considered are two-dimensional; hence, their cross-sectional geometry remains constant along one of the space directions.

Thus, the calculated capacitances are per unit length. For the first three examples, the orthogonal polynomial chaos expansion is used while a Monte Carlo approach is used for the last example.

3.3.1 Example 1: Single conductor over a ground plane

We consider a rectangular strip conductor embedded in a three-layer substrate above a ground plane. The problem consists of determining the effect of variations in conductor width, L , and its distance from the ground plane, H , on per-unit-length capacitance. The mean dimensions and the material properties of the cross-sectional geometry are specified in Fig. 3.3(a).

First, we consider the distance from the ground, H , to be a random variable, and express it as

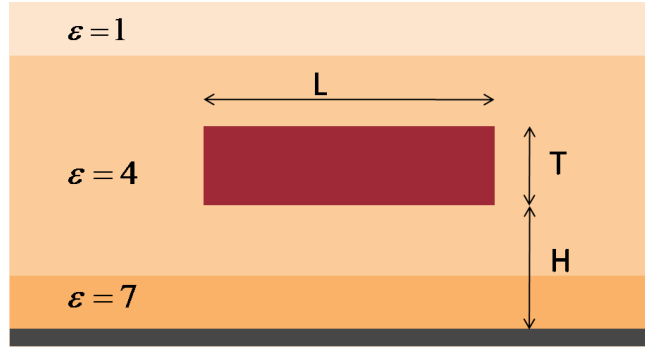
$$H(\theta) = H_0(1 - \nu\xi(\theta)) \quad (3.32)$$

where $H_0 = 0.2 \mu\text{m}$ is the mean or average distance, ξ is a Gaussian random variable with unit variance and ν is the variation in H . This, basically, may be considered as a random displacement, $\nu\xi(\theta)H_0$, applied to the conductor at mean height H_0 above ground. Following (3.20),(3.27)-(3.29),

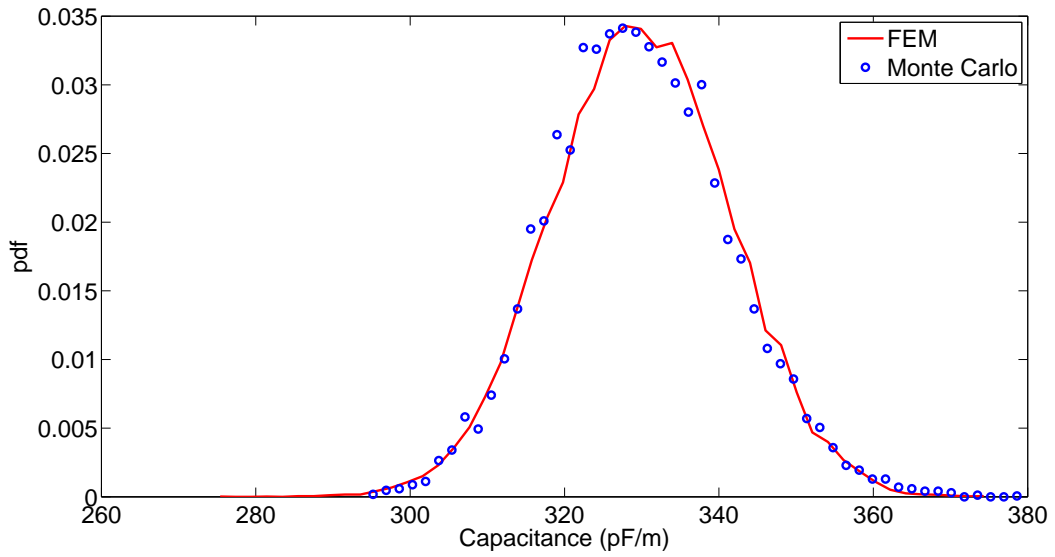
$$v(\vec{r}, \theta) = \nu\xi H_0 \quad (3.33)$$

$$\tilde{C} = \int_S \left(1 + \left(\frac{\nu H_0}{G(\vec{r})} \right) \xi + \left(\frac{\nu H_0}{G(\vec{r})} \right)^2 \xi^2 + \dots \right) |J| |\vec{D}_0| dl \quad (3.34)$$

$G(\vec{r})$ is the position-dependent flux length as defined in (3.8). Using up to quadratic terms



(a)



(b)

Figure 3.3: (a) One conductor over a ground plane. (b) Probability distribution function of the capacitance for a 10% variation in distance from ground plane.

in the expansion for stochastic capacitance,

$$\tilde{C} = C_0 + C_1\xi + C_2(\xi^2 - 1) \quad (3.35)$$

Then, the coefficients can be obtained from

$$C_0 = \int_S \left(1 + \left(\frac{\nu H_0}{G(\vec{r})} \right)^2 \right) |J| |\vec{D}_0| dl \quad (3.36)$$

$$C_1 = \int_S \left(\frac{\nu H_0}{G(\vec{r})} \right) |J| |\vec{D}_0| dl \quad (3.37)$$

$$C_2 = \int_S \left(\frac{\nu H_0}{G(\vec{r})} \right)^2 |J| |\vec{D}_0| dl \quad (3.38)$$

Since the volume of the geometry does not change, $|J| = 1$. $G(\vec{r})$ and $|\vec{D}_0|$ are obtained from the solution of the deterministic problem in the mean geometry. Thus, only one deterministic problem needs to be solved. The mean of the capacitance is given by C_0 , while the standard deviation is given by $\sqrt{C_1^2 + 2C_2^2}$.

We use standard Monte Carlo method for generating the reference solution. In the standard Monte Carlo approach we consider a number of realizations of the random geometry and carry out a finite element solution for each geometry to compute capacitance. To obtain the pdf of capacitance depicted in Fig. 3.3(b) (for 10% change in gap), 10 000 solutions were used. The mean and standard deviation obtained with our proposed method is in close agreement with that obtained using Monte Carlo (Table 3.1). Note that performing 10 000 simulations took approximately 15 000 seconds. This is in contrast to the 2 seconds required by the proposed alternative approach.

We repeat this exercise for random variation in the conductor width L and the results are summarized in Table 3.2. Once again, the results show that our proposed method is very accurate and extremely efficient.

Table 3.1: Example 1 (self-capacitance in pF/cm): Statistical change in G

%change in H	Monte Carlo		Proposed method	
	mean	std. dev	mean	std. dev
10%	3.29	0.115	3.29	0.114
20%	3.31	0.236	3.31	0.233

Table 3.2: Example 1 (self-capacitance in pF/cm): Statistical change in L

%change in L	Monte Carlo		Proposed method	
	mean	std. dev	mean	std. dev
10%	3.31	0.073	3.29	0.075
20%	3.31	0.15	3.29	0.15

3.3.2 Example 2: Strip conductor interconnect in a multi-layered dielectric substrate

For this example we consider, once again, a strip interconnect embedded in a multi-layered insulating substrate. Fig. 3.4 describes the geometric and material properties of the cross-sectional geometry. The objective is to investigate the impact of variations in thicknesses of the insulating layers on the per-unit-length capacitance of the structure. The procedure for modeling uncertainty is similar to that described in Example 1 and will not be repeated here. Shown in Table 3.3 is a comparison between our approach and standard Monte Carlo for mean and standard deviation of capacitance. The results demonstrate the accuracy of the proposed approach.

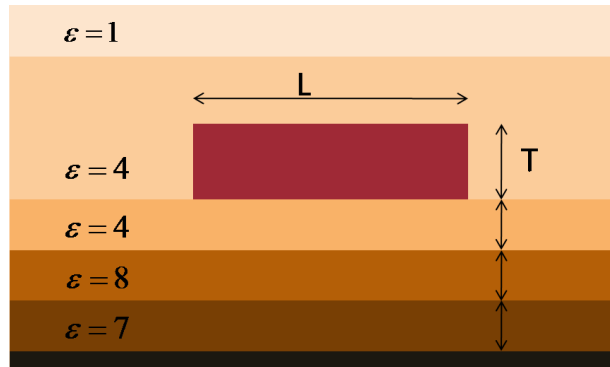


Figure 3.4: Strip conductor embedded in multiple dielectrics.

Table 3.3: Example 2 (self-capacitance in pF/cm): Statistical change in thicknesses

%change in thickness for each layer	Monte Carlo		Proposed method	
	mean	std. dev	mean	std. dev
10%	2.68	0.067	2.68	0.063
20%	2.69	0.135	2.67	0.125

3.3.3 Example 3: Two strip conductors over a ground plane

In this example we consider two conductors over a ground plane. The dielectric properties of the multi-layered substrate are similar to those in Example 1. The specific details of the cross-sectional geometry and material parameters are shown in Fig. 3.5. The objective in this example is to investigate the combined impact of variations in height above ground and spacing between the two conductors on the self-capacitance of one of the conductors. Table 3.4 summarizes the results for 10% and 20% variation in these parameters.

Once again, the comparison of results obtained using the proposed method with those generated through a standard Monte Carlo approach demonstrates the accuracy of the proposed method.

Table 3.4: Example 3 (self-capacitance in pF/cm): Statistical change in H and S

%change in H and S	Monte Carlo		Proposed method	
	mean	std. dev	mean	std. dev
10%	3.68	0.13	3.68	0.14
20%	3.70	0.26	3.70	0.28

3.3.4 Example 4: A three-conductor interconnect over a ground plane

In this example, we consider three conductors over a ground plane. The details of the cross-sectional geometric and material parameters are shown in Fig. 3.6. The objective in this example is to investigate the combined impact of variations in heights H_1 (mean 0.2) and H_2

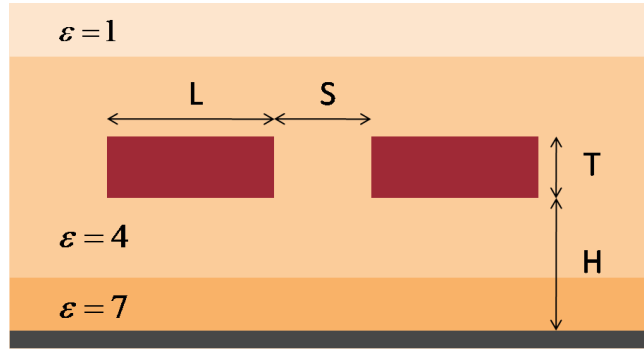


Figure 3.5: Two conductors over a ground plane.

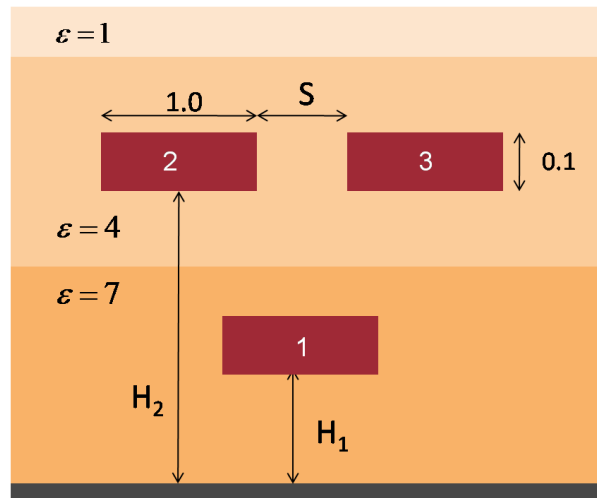


Figure 3.6: Three conductors over a ground plane.

(mean 0.5) above ground and spacing between the two conductors S (mean 2.0). One could use a polynomial chaos expansion approach as used in the previous examples. However, since three random variables are involved, the form of the expansion becomes complicated. Thus, we consider, instead, an alternative implementation using Monte Carlo as was described in Section 3.2. In this, we consider 10 000 Monte Carlo random samples of the geometry. For standard Monte Carlo, we use a finite element solution for each random realization, whereas for the proposed approach we carry out a single finite element solution on the mean geometry only, along with displacements of random samples from the mean geometry. Table 3.5 summarizes the results for mean capacitance matrix for 10% variation in these

parameters. Table 3.6 summarizes the results for standard deviation for self-capacitance. Once again, the comparison of the results obtained using the two approaches demonstrates the accuracy of the proposed method.

Table 3.5: Example 4: Mean capacitance in pF/cm using standard Monte Carlo and our proposed approach

	Monte Carlo			Proposed method		
	1	2	3	1	2	3
1	4.66	-0.222	-0.227	4.68	-0.226	-0.226
2	-0.222	1.84	-0.013	-0.226	1.84	-0.013
3	-0.227	-0.013	1.84	-0.226	-0.013	1.84

Table 3.6: Example 4: Standard deviation of self-capacitance in pF/cm using standard Monte Carlo and our proposed approach

	Monte Carlo	Proposed method
C_{11}	0.116	0.111
C_{22}	0.082	0.078
C_{33}	0.082	0.079

3.4 Summary

In summary, we have proposed a method for expediting the stochastic extraction of interconnect capacitance. This was accomplished through the development of a “mapping” from a random sample to a mean geometry. This mapping is developed through the approximate calculation of charge density on the conductor in the random geometry in terms of charge density in the mean geometry. This definition is based on the ratio of two line integrals. The line integrals involve a displacement, which is interpreted as a displacement of the random geometry from the mean geometry.

The accuracy and efficiency of the proposed method were demonstrated through its

application to a few representative examples of capacitance extraction for interconnects in multi-layer dielectrics. The proposed approach was shown to be more than three orders of magnitude faster than a standard Monte Carlo approach.

Finally, we would like to comment on the versatility of the proposed method. The proposed “mapping” is independent of which particular approach is used for representing randomness in the geometry. More specifically, it was shown that the proposed method can be coupled with both polynomial chaos expansion based approaches and statistical approaches such as Monte Carlo or stochastic collocation.

References

- [1] N. Agarwal and N.R. Aluru. A stochastic Lagrangian approach for geometrical uncertainties in electrostatics. *Journal of Computational Physics*, 226:156–179, 2007.
- [2] N. Agarwal and N.R. Aluru. Stochastic modeling of coupled electromechanical interaction for uncertainty quantification in electrostatically actuated MEMS. *Computer Methods in Applied Mechanics and Engineering*, 197:3456–3471, 2008.
- [3] N. Agarwal and N.R. Aluru. A domain adaptive stochastic collocation approach for analysis of MEMS under uncertainties. *Journal of Computational Physics*, 228:7662–7688, 2009.
- [4] R. Ananthakrishna and S. Batterywala. MoM - a process variation aware statistical capacitance extractor. *Proc. International Conference on VLSI Design*, pages 135–140, 2006.
- [5] N.D. Arora, K.V. Raol, R. Schumann, and L.M. Richardson. Modeling and extraction of interconnect capacitances for multilayer VLSI circuits. *IEEE Transactions on Computer-Aided Design*, 15:58–67, 1996.
- [6] M. Berkelaar. Statistical delay calculation, a linear time method. *Proc. International Workshop on Timing Issues in the Specification and Synthesis of Digital Systems (TAU)*, pages 15–24, 1997.
- [7] Cadence. <http://www.cadence.com>, accessed Jan 2010.
- [8] C. Chauvere, J. S. Hesthaven, and L. Lurati. Computational modeling of uncertainty in time domain electromagnetics. *SIAM Journal of Scientific Computing*, 28:751–775, 2006.
- [9] P. E. Cottrell and E. M. Buturla. VLSI wiring capacitance. *IBM Journal of Research and Development*, 29:277–288, 1985.
- [10] Y. Le Coz, H. Greub, and R. Iverson. Performance of random walk capacitance extractors for IC interconnects: a numerical study. *Solid State Electronics*, 42:581–588, 1998.
- [11] J. Cui, G. Chen, R. Shen, S. X.-D. Tan, W. Yu, and J. Tong. Variational capacitance modeling using orthogonal polynomial method. *Proc. IEEE/ACM International Great Lakes Symposium on VLSI (GLSVLSI08)*, pages 23–28, 2008.

- [12] G. S. Fishman. *Monte Carlo: Concepts, Algorithms, and Applications*. Springer-Verlag, New York, 1996.
- [13] B. Fox. *Strategies for Quasi-Monte Carlo*. Kluwer, The Netherlands, 1999.
- [14] R. Ghanem and P. Spanos. *Stochastic Finite Elements: A Spectral Approach*. Springer, New York, 1991.
- [15] W. Gilks, S. Richardson, and D. Spiegelhalter. *Markov Chain Monte Carlo in Practice*. Chapman & Hall, London, 1995.
- [16] F. Gong, H. Yu, and L. He. PiCAP: A parallel and incremental capacitance extraction considering stochastic process variation. *Proc. of the 46th Annual Design Automation Conference*, pages 764–769, 2009.
- [17] R. Guerrieri and A. L. Sangiovanni-Vincentelli. Three-dimensional capacitance evaluation on a connection machine. *IEEE Transactions on Computer-Aided Design*, 7:1125–1133, 1988.
- [18] M. Hashimoto, M. Takahashi, and H. Onodera. Crosstalk noise estimation for generic RC trees. *IEICE Transactions on Fundamentals of Electronics*, E86-A:2965–2973, 2003.
- [19] F. Huebbers, A. Dasdan, and Y. Ismail. Computation of accurate interconnect process parameter values for performance corners under process variations. *Proc. Design Automation Conference*, pages 797–800, 2006.
- [20] R. Iverson and Y. Le Coz. A floating random-walk algorithm for extracting electrical capacitance. *Mathematics and Computers in Simulation*, 55:59–66, 2001.
- [21] R. Jiang, W. Fu, J. M. Wang, V. Lin, and C. C.-P. Chen. Efficient statistical capacitance variability modeling with orthogonal principle factor analysis. *Proc. International Conference on Computer Aided Design (ICCAD)*, pages 683–690, 2005.
- [22] T. Kanamoto, T. Watanabe, M. Shirota, M. Terai, T. Kunikiyo, K. Ishikawa, Y. Ajioka, and Y. Horiba. A method of precise estimation of physical parameters in LSI interconnect structures. *IEICE Transactions on Fundamentals of Electronics*, E88-A:3463–3470, 2005.
- [23] W. Loh. On Latin hypercube sampling. *Annals of Statistics*, 24:2058–2080, 1996.
- [24] Mentor Graphics. <http://www.mentor.com>, accessed Jan 2010.
- [25] K. Nabors and J. White. Fastcap: a multipole accelerated 3-d capacitance extraction program. *IEEE Transactions on Computer Aided Design*, 10:1447–1459, 1991.
- [26] H. Niederreiter. *Random Number Generation and Quasi-Monte Carlo Methods*. SIAM, Philadelphia, 1992.
- [27] H. Niederreiter, P. Hellekalek, G. Larcher, and P. Zinterhof. *Monte Carlo and Quasi-Monte Carlo Methods*. Springer-Verlag, New York, 1998.

- [28] J. Singh and S. Sapatnekar. Statistical timing analysis with correlated non-Gaussian parameters using independent component analysis. *Proc. Design Automation Conference*, pages 155–160, 2006.
- [29] S. Smolyak. Quadrature and interpolation formulas for tensor products of certain classes of functions. *Soviet Mathematics Doklady*, 4:240–243, 1963.
- [30] M. Stein. Large sample properties of simulations using Latin hypercube sampling. *Technometrics*, 29:143–151, 1987.
- [31] P. S. Sumant, N. R. Aluru, and A. C. Cangellaris. A methodology for fast finite element modeling of electrostatically actuated MEMS. *International Journal for Numerical Methods in Engineering*, 77:1789–1808, 2009.
- [32] P.S. Sumant and A.C. Cangellaris. Algebraic multigrid Laplace solver for the extraction of capacitances of conductors in multi-layer dielectrics. *International Journal of Numerical Modelling: Electronic Networks, Devices and Fields*, 20:253–269, 2007.
- [33] Synopsys. <http://www.synopsys.com/home.aspx>, accessed Jan 2010.
- [34] D. Xiu and Jan S. Hesthaven. Higher order collocation methods for differential equations with random inputs. *SIAM Journal of Scientific Computing*, 27:1118–1139, 2005.
- [35] D. Xiu and G.E. Karniadakis. Modeling uncertainty in steady state diffusion problems via generalized polynomial chaos. *Computer Methods in Applied Mechanics and Engineering*, 191:4927–4948, 2002.
- [36] D. Xiu and G.E. Karniadakis. Modeling uncertainty in flow simulations via generalized polynomial chaos. *Journal of Computational Physics*, 187:137–167, 2003.
- [37] W. Zhang, W. Yu, Z. Wang, Z. Yu, R. Jiang, and J. Xiong. An efficient method for chip-level statistical capacitance extraction considering process variations with spatial correlation. *Proc. European Design and Test Conference (DATE)*, pages 580–585, 2008.
- [38] H. Zhu, X. Zeng, W. Cai, and D. Zhou. A spectral stochastic collocation method for capacitance extraction of interconnects with process variations. *Proc. of IEEE Asia Pacific Conference on Circuits and Systems*, pages 1095–1098, 2006.
- [39] Z. Zhu, J. White, and A. Demir. A stochastic integral equation method for modeling the rough surface effect on interconnect capacitance. *Proceedings of the 2004 IEEE/ACM International Conference on Computer-aided Design*, pages 887–891, 2004.

Author's Biography

Prasad S. Sumant received his B.Tech. (Bachelor of Technology) in Mechanical Engineering and M.Tech. (Master of Technology) in Computer Aided Design and Automation (CADA) from the Indian Institute of Technology Bombay (IITB), India, in 2004. Upon graduation, he joined Asian Paints India Ltd. as a management trainee. He joined the Department of Mechanical Science and Engineering at the University of Illinois at Urbana-Champaign (UIUC) in Fall 2005. He is currently working toward his Ph.D. degree. In addition, he is also pursuing an M.S. in Electrical and Computer Engineering. His research interests include computational methods for design and analysis of MEMS, computational electromagnetics, numerical techniques in engineering, stochastic modeling and scientific computing. He is a recipient of the Outstanding Scholar Fellowship (2005-present) from the Department of Mechanical Science and Engineering at UIUC. He was elected to the honor society of Phi Kappa Phi in 2007 and Tau Beta Pi in 2009. Upon graduation, Prasad will be joining ExxonMobil Upstream Research Company as a research engineer.